Article:
Graham, A.I., Hunt, S., Stokes, S.L. et al. (5 more authors) (2009) Severe zinc depletion of escherichia coli: roles for high affinity zinc binding by ZinT, zinc transport and zinc-independent proteins. Journal of Biological Chemistry, 284 (27). pp. 18377-18389. ISSN 0021-9258

https://doi.org/10.1074/jbc.M109.001503

SEVERE ZINC DEPLETION OF ESCHERICHIA COLI: ROLES FOR HIGH-AFFINITY ZINC BINDING BY ZinT, ZINC TRANSPORT AND ZINC-INDEPENDENT PROTEINS

Alison I. Graham[1], Stuart Hunt[1], Sarah L. Stokes[2], Neil Bramall[2], Josephine Bunch[2#], Alan G. Cox[2], Cameron W. McLeod[2] and Robert K. Poole[1*]

[1]Department of Molecular Biology and Biotechnology and [2]Centre for Analytical Sciences, The University of Sheffield, Western Bank, Sheffield, S10 2TN, UK

Running title: Transcriptional response to zinc limitation

Address correspondence to: Robert Poole, Department of Molecular Biology and Biotechnology The University of Sheffield, Western Bank, Sheffield, S10 2TN, UK; Telephone (0)114 222 4447; Fax (0)114 222 2800; E-mail r.poole@sheffield.ac.uk.

Present address: School of Chemistry, University of Birmingham, Edgbaston, Birmingham, B15 2TT, UK.

Zinc ions play indispensable roles in biological chemistry. However, bacteria have an impressive ability to acquire Zn^{2+} from the environment, making it exceptionally difficult to achieve Zn^{2+} deficiency and so a comprehensive understanding of the importance of Zn^{2+} has not been attained. Reduction of the Zn^{2+} content of Escherichia coli growth medium to 60 nM or less is reported here for the first time, without recourse to chelators of poor specificity. Cells grown in Zn^{2+}-deficient medium had a reduced growth rate and contained up to five times less cellular Zn^{2+}. To understand global responses to Zn^{2+} deficiency, microarray analysis was conducted of cells grown under Zn^{2+}-replete and Zn^{2+}-depleted conditions in chemostat cultures. Nine genes were up-regulated more than two-fold ($P<0.05$) in cells from Zn^{2+}-deficient chemostats, including zinT (yodA). zinT is shown to be regulated by Zur (zinc uptake regulator). A mutant lacking zinT displayed a growth defect and a three-fold lowered cellular Zn^{2+} level under Zn^{2+} limitation. The purified ZinT protein possessed a single, high-affinity metal-binding site which can accommodate Zn^{2+} or Cd^{2+}. A further up-regulated gene, ykgM, is believed to encode a non-Zn^{2+}-finger-containing paralogue of the Zn^{2+}-finger ribosomal protein L31. The gene encoding the periplasmic Zn^{2+}-binding protein znuA showed increased expression. During both batch and chemostat growth, cells "found" more Zn^{2+} than was originally added to the culture, presumably due to leaching from the culture vessel. Zn^{2+} elimination is shown to be a more precise method of depleting Zn^{2+} than by using the chelator N, N, N`, N`-tetrakis(2-pyridylmethyl)ethylenediamine (TPEN).

Almost all biological interactions depend upon contacts between precisely structured protein domains and Zn^{2+} may be used to facilitate correct folding and stabilize the domain (1,2). Zn^{2+} also plays an indispensable catalytic role in many proteins (1). Although normally classed as a trace element, Zn^{2+} accumulates to the same levels as Ca and Fe in the Escherichia coli cell (3); predicted Zn^{2+}-binding proteins account for 5-6% of the total proteome (4).

However, despite its indispensable role in biology, as with all metals, Zn^{2+} can become toxic if accumulated to excess. With no sub-cellular compartments to deposit excess metal, Zn^{2+} homeostasis in bacteria relies primarily on tightly regulated import and export mechanisms (5). The major inducible high-affinity Zn^{2+} uptake system is the ABC transporter, ZnuABC. ZnuA is important for growth (6) and Zn^{2+} uptake (7) and is thought to pass Zn^{2+} to ZnuB for transport through the membrane. Zn^{2+}-bound Zur represses transcription of znuABC, whilst addition of the metal chelator N, N, N`, N`-tetrakis(2-pyridylmethyl)ethylenediamine (TPEN)

de-represses expression from a promoterless lacZ gene inserted into znuA, znuB and znuC (8). Zur can sense sub-femtomolar concentrations of cytosolic Zn^{2+}, implying that cellular Zn^{2+} starvation commences at exceptionally low Zn^{2+} concentrations (3). Outten and O'Halloran (3) found that the minimal Zn^{2+} content required for growth in E. coli is 2×10^5 atoms per cell, which corresponds to a total cellular Zn^{2+} concentration of 0.2 mM, approximately 2000 times the Zn^{2+} concentration found in the medium. A similar cellular concentration of Zn^{2+} was found in cells grown in Luria-Bertani medium (LB).

Thus, E. coli has an impressive ability to acquire and concentrate Zn^{2+} (3), making the task of depleting this organism of Zn^{2+} very difficult. Nevertheless, during the course of this work, a paper was published (9) in which the authors conclude that ZinT (formerly YodA) "is involved in periplasmic zinc binding and either the subsequent import or shuttling of zinc to periplasmic zinc-containing proteins under zinc-limiting conditions". Surprisingly, this conclusion was drawn from experiments in which Zn^{2+} levels in the medium were lowered only by reducing the amount of Zn^{2+} added, without metal extraction or chelation.

Only a few attempts have been made to study the global consequences of metal deficiency using "omic" technologies. A study using TPEN (10) found 101 genes to be differentially-regulated in E. coli. However, the authors note that TPEN has been reported to bind Cd^{2+}, Co^{2+}, Ni^{2+} and Cu^{2+} more tightly than it binds Zn^{2+} and, indeed, 34 of the 101 differentially-regulated genes are transcriptionally regulated by Fur (the Fe-uptake regulator) or involved in Fe or Cu metabolism. Thus the transcriptome of E. coli associated with Zn^{2+} deficiency alone has not been elucidated. Most genome-wide microarray studies of the effects of metal stresses to date have been carried out in batch culture, but continuous culture offers major benefits for such studies. The greater biological homogeneity of continuous cultures and the ability to control all relevant growth conditions, such as pH and especially growth rate, eliminate the masking effects of secondary stresses and growth rate changes, allowing more precise delineation of the response to an individual stress (11,12). In the case of transcriptomics, it has been demonstrated that the reproducibility of analyses between different laboratories is greater when chemostat cultures are used than when identical analyses are performed with batch cultures (13). Some studies have exploited continuous culture to examine the effects of metal stresses such as that of Lee et al. (14) in which E. coli cultures grown in continuous culture at a fixed specific growth rate, temperature and pH were used to assay the transcriptional response to Zn^{2+} excess. In the present study, E. coli was grown in continuous culture in which severe depletion was achieved without recourse to chelating agents in the medium by thorough extraction and scrupulous attention to metal contamination. Microarray analysis identifies only nine genes that respond significantly to Zn^{2+} starvation. We demonstrate here for the first time that one such gene, zinT, is up-regulated in response to extreme Zn^{2+} deprivation by Zur, and that ZinT has a high affinity for Zn^{2+}. We also reveal roles for Zn^{2+} re-distribution in surviving Zn^{2+} deficiency.

EXPERIMENTAL PROCEDURES

Bacterial strains and growth conditions - Bacterial strains used in this study are listed in Table 1. Cells were grown in glycerol-glycerophosphate medium (GGM), slightly modified from Beard et al. (15). GGM is buffered with 2-(N-morpholino)ethanesulfonic acid (MES), which has minimal metal-chelating properties, and uses organic phosphate as the phosphate source to minimise formation of insoluble metal phosphates (16). Final concentrations are: MES (40.0

mM), NH_4Cl (18.7 mM), KCl (13.4 mM), β-glycerophosphate (7.64 mM), glycerol (5.00 mM), K_2SO_4 (4.99 mM), $MgCl_2$ (1.00 mM), EDTA (134 μM), $CaCl_2.2H_2O$ (68.0 μM), $FeCl_3.6H_2O$ (18.5 μM), ZnO (6.14 μM), H_3BO_3 (1.62 μM), $CuCl_2.2H_2O$ (587 nM), $Co(NO_3)_2.6H_2O$ (344 nM), and $(NH_4)_6Mo_7O_{24}.4H_2O$ (80.9 nM) in MilliQ water (Millipore). Bulk elements (MES, NH_4Cl, KCl, K_2SO_4 and glycerol in MilliQ water at pH 7.4 (batch growth) or 7.6 (continuous culture)) were passed through a column containing Chelex-100 ion exchange resin (Bio-Rad) to remove contaminating cations. Trace elements (with or without Zn^{2+} as necessary) and a $CaCl_2$ solution were then added to give the final concentrations shown above prior to autoclaving. After autoclaving, $MgCl_2$ and β-glycerophosphate were added at the final concentrations shown. All chemicals were of AnalaR grade purity or higher. Chelex-100 was packed into a Bio-Rad Glass Econo-column (approximately 120 mm × 25 mm) that had previously been soaked in 3.5% nitric acid for 5 d.

Creating Zn^{2+}-deficient conditions and establishing Zn^{2+}-limited cultures - Culture vessels and medium were depleted of Zn^{2+} by extensive acid-washing of glassware, the use of a chemically-defined minimal growth medium, chelation of contaminating cations from this medium using Chelex-100, and the use of newly-purchased high-purity chemicals and metal-free pipette tips. Plastics that came into contact with the medium (e.g. bottles, tubes, tubing) were selected on the basis of their composition and propensity for metal leaching, and included polypropylene, polyethylene, polytetrafluoroethylene (PTFE) or polyvinyl chloride (PVC). Dedicated weigh boats, spatulas, measuring cylinders, PTFE-coated stir bars and a pH electrode were used. PTFE face masks, polyethylene gloves and a PTFE-coated thermometer were also used. Solutions were filter-sterilised using polypropylene syringes with no rubber seal, in conjunction with syringe filters with a PTFE membrane and polypropylene housing. Vent filters contained a PTFE membrane in polypropylene housing. Cells were grown in continuous culture in a chemostat that was constructed entirely of non-metal parts as detailed below.

Continuous culture of E. coli strain MG1655 - E. coli strain MG1655 was grown in custom-built chemostats made entirely of non-metal parts essentially as in Lee et al. (14) with some modifications. Glass growth vessels and flow-back traps were soaked extensively (approximately two months) in 10% nitric acid before rinsing thoroughly in MilliQ water. Vent filters (Vent Acro 50 from VWR) were connected to the vessel using PTFE tubing. Metal-free pipette tips were used (MAXYMum Recovery Filter Tips from Axygen). Culture volume was maintained at 120 ml using an overflow weir in the chemostat vessel (14). The vessel was inoculated using one of the side-arms. Flasks were stirred on KMO 2 Basic IKA-Werke stirrers at 437 rpm determined using a handheld laser tachometer (Compact Instruments Ltd). The use of a vortex impeller suspended from above the culture avoided grinding of the glass vessel that would occur if a stir bar were used. Samples were taken from the culture vessel as in Lee et al. (14). The dilution rate (and hence the specific growth rate) was 0.1 h^{-1} (which is below the maximal specific growth rate μ_{max} for this strain (17)). No washout was observed in long-term chemostat cultures in Zn^{2+}-depleted medium. One chemostat was fed medium that contained "adequate" Zn^{2+} (i.e. normal GGM concentration), whilst the other contained no added Zn^{2+} and had been depleted of Zn^{2+} as above. Chemostats were grown for 50 h to allow five culture volumes to pass through the vessel and allow an apparent (pseudo-)steady state to be reached. More prolonged growth was avoided to minimise the formation of mutations in the rpoS gene (18). Samples were taken throughout to check pH, OD_{600}, glycerol content and for contaminants.

Steady state values for pH and OD_{600} were 6.9 and 0.6, respectively. Glycerol assays (19) showed cultures to be glycerol-limited.

The "Zn^{2+}-free" chemostat was inoculated with cells that had been sub-cultured in Zn^{2+}-free medium. A 0.25 ml aliquot of a saturated culture of strain MG1655 grown in LB was centrifuged and the pellet used to inoculate 5 ml of GGM that was incubated overnight at 37 ^{o}C with shaking. A 2.4 ml (i.e. 2% of chemostat volume) aliquot of this was then used to inoculate the chemostat. The "adequate Zn^{2+}" chemostat was inoculated with cells treated in essentially the same way but grown in GGM containing "adequate" Zn^{2+}. The two cultures (+/- Zn^{2+}) used to inoculate the chemostats had OD_{600} readings within 2.5% of each other. Aliquots from the chemostat were used to harvest RNA and for metal analysis by inductively coupled plasma-atomic emission spectroscopy (ICP-AES, see below).

Batch growth of E. coli strains in GGM +/- Zn^{2+} - A saturated culture was grown in LB (with antibiotics as appropriate). To minimise carry-over of broth, cells were collected from approximately 0.25 ml culture by centrifugation and the pellet resuspended in a 5 ml GGM starter culture (with Zn^{2+} and antibiotics as appropriate) for 24 h. Side-arm flasks containing 25 ml GGM with Zn^{2+} were then inoculated with the equivalent of 1 ml of a culture with OD_{600} of 0.6. For these experiments, "plus Zn" cultures were grown in medium containing adequate Zn^{2+} where no special precautions were taken in preparing the medium. "Zn-depleted" cultures were grown in side-arm flasks that had been soaked extensively in 10% nitric acid before rinsing thoroughly in MilliQ water. Growth was measured over several hours using a Klett colorimeter and a red filter (number 66; Manostat Corporation). The colorimeter was blanked using GGM. No antibiotics were present in the growth medium used for batch growth curves as they can act as chelators (20-23), but cultures were spotted onto solid LB plates with and without antibiotics at the end of the growth curve to verify that antibiotic resistance was retained. At the end of the growth curve, aliquots of the culture were combined and pelleted for ICP-AES analysis (see below).

RNA isolation and microarray procedures - These were conducted as described by Lee et al. (14). RNA was quantified using a BioPhotometer (Eppendorf). E. coli K-12 V2 OciChip microarray slides were purchased from Ocimum Biosolutions Ltd (previously MWG Biotech). Biological experiments (i.e. comparison of low Zn^{2+} versus adequate Zn^{2+} in chemostat culture) were carried out three times, and a dye swap performed for each experiment, providing two technical repeats for each of the three biological repeats. Data were analysed as before (14). Spots automatically flagged as bad, negative or poor in the Imagene software were removed before the statistical analysis was carried out in GeneSight.

zinT gene inactivation - The zinT gene was functionally inactivated by the insertion of a chloramphenicol resistance cassette using the method of Datsenko and Wanner (24). The pACYC184 chloramphenicol resistance cassette was amplified by PCR using primers that have 40 bases of identity at their 5' ends to regions within the zinT gene. The forward primer was 5'-GCATGGTCATCACTCACACGGCAAA CCCTTAACAGAGGTCAAGCCACTGG AGCACCTCAA-3' and the reverse was 5'-CAATGCCGTCCTCAATGCCAATCAT CTCGATATCTGTTGCACGGGGAGAG CCTGAGCAAA-3' (regions homologous to zinT are underlined). The linear DNA was used to transform strain RKP5082 by electroporation. This strain contains pKD46 which over-expresses the phage λ recombination enzymes when arabinose is present. Bacteria were grown to an OD_{600} of 0.6 in 500 ml LB containing ampicillin (150 μg/ml final concentration) and arabinose (1 mM final concentration) at 30

^{o}C. Cells were then pelleted and made electrocompetent by washing the pellet three times in ice-cold 10% glycerol. The last pellet was not resuspended but vortexed into a slurry. Aliquots of cells (50-100 µl) were electroporated with 1-10% linear DNA (v:v) at 1800 V. Cells were recovered by the addition of 1 ml of LB and incubation at 37 ^{o}C for 90 min. Cells were then pelleted and plated onto LB containing chloramphenicol at 34 µg/ml (final concentration). Loss of pKD46 plasmid was checked by streaking transformants on LB agar plates containing ampicillin (150 µg/ml final concentration). Insertion of the chloramphenicol cassette was checked by DNA sequencing. The zinT::cam mutant strain was named RKP5456.

Construction of a $\lambda\Phi$(P_{zinT}-lacZ) zur::Spc^{r} strain - The zur::Spc^{r} mutation in strain SIP812 (8) was moved into strain AL6, which harbours the λΦ(P_{zinT}-lacZ) fusion (25), by P1 transduction (26). The strain was named RKP5475.

Quantitative real-time-polymerase chain reaction (qRT-PCR) - This was carried out on RNA samples harvested from the chemostats exactly as described in Lee et al. (14). The mRNA levels of holB were unchanged as determined by array analysis and were thus used as an internal control.

ICP-AES - Cells (from 25 ml culture (batch) or approximately 85 ml (chemostat)) were harvested by centrifugation at 5000 × g for 5 min (Sigma 4K15) in polypropylene tubes from Sarstedt (catalogue numbers 62.547.004 (50 ml) or 62.554.001 (15 ml)). Culture supernatants were retained for analysis. Pellets were washed three times in 0.5 ml of 0.5 % HNO_3 (Aristar nitric acid, 69% v/v) to remove loosely bound elements. Supernatants collected from the washes were also retained for analysis.

Pellets were resuspended in 0.5 ml HNO_3 (69%) before transfer to nitric acid-washed test tubes (previously dried). The samples were placed in an ultrasonic bath for approximately 30 min to break the cells. The resultant digest was then quantitatively transferred to a calibrated 15 ml tube and made up to 5 ml with 1% HNO_3. Samples were analysed using a Spectrociros^{CCD} (Spectroanalytical) inductively coupled plasma-atomic emission spectrometer using background correction. Analyte curves were created for each element to be tested using multi-element standard solutions containing 0.1, 0.2, 1, 5 and 10 mg l^{-1}. The wavelengths (nm) for each element were as follows: Ca, 183.801; Co, 228.616; Cu, 324.754 and 327.396; Fe, 259.941; Mg, 279.079; Mo, 202.030; Na, 589.592; Zn, 213.856. A 1% nitric acid solution in MilliQ water was used as a blank and to dilute cell digests before ICP-AES analysis. Concentrations of each element in each sample (pellets, culture supernatants and wash supernatants) were calculated using the standard curves. Measurements obtained were the mean of five replicate integrations. The limit of Zn^{2+} detection was 0.001 mg l^{-1} (i.e. 1 ppb). In the "simple" low-matrix solutions analysed here, the wavelength used for Zn^{2+} detection is interference-free and specific for Zn^{2+}.

Elemental recoveries were calculated from these samples. Two different recovery calculations were performed: 1) the percentage of an element in the culture that was subsequently recovered in the washed cell pellet, wash supernatants and culture supernatant, and 2) the percentage of an element recovered in the unwashed pellet and culture supernatant. The former was used for batch and chemostat samples and the latter for chemostat only. In some samples, element concentrations were below the calculated limit of detection (LOD) for the method. LOD is calculated from the calibration curve based on three σ of a blank signal. Where the signal is at or below the LOD, the instrument reports a <LOD value. In these cases, the LOD is used in subsequent calculations so will be an over-estimation. Detection of Zn^{2+} was

further complicated because, in many cases, Zn^{2+} concentrations were close to unavoidable background levels.

Calculation of dry cell weight – Cellular metal contents were expressed on a dry cell mass basis. This was determined by filtering known volumes of culture (10 ml, 20 ml and 30 ml) through pre-weighed cellulose nitrate filters, 47 mm diameter and pore size 0.2 μm (Millipore). The filters had previously been dried at 105 ^{o}C for 18-24 h to constant weight. The filters were again dried at 105 ^{o}C until a constant weight was attained, which was recorded.

β-galactosidase activity assay - For β-galactosidase assays with strains AL6 ($\lambda\Phi(P_{zinT}$-lacZ)) and RKP5475, a saturated culture was grown in LB with or without spectinomycin (50 μg/ml final concentration) as appropriate and cells from approximately 0.25 ml culture collected and resuspended in 5 ml GGM with or without Zn^{2+} and spectinomycin as appropriate. This was incubated overnight at 37 ^{o}C with shaking. A 1 ml aliquot of this was then used to inoculate several cultures (15 ml) as described in the text. Cultures were harvested when an OD_{600} of 0.2-0.4 was reached. Immediately prior to harvesting, 5 μl was spotted onto solid LB plates with and without antibiotics to check that resistance was retained. Separate flasks were set up and used to grow the strains under each of the conditions mentioned above for ICP-AES analysis.

β-galactosidase activity was measured in $CHCl_3$- and SDS-permeabilized cells by monitoring the hydrolysis of o-nitrophenyl-β-D-galactopyranoside. Cell pellets were resuspended in approximately 15 ml Z buffer (26). Each culture was assayed in triplicate. Absorbance (A) at 420 nm, 550 nm and 600 nm was measured to allow β-galactosidase activity (Miller units) to be calculated as (26).

Cloning of zinT for protein purification - Primers 5'-CTCCTGCCTTTCATATGGGTCATCA C-3' (forward) and 5'-CATAGTGATGAGCTCGTCTGTAGC-3' (reverse) were used to amplify the zinT coding region minus the sequence that encodes the 24-amino acid periplasmic signalling sequence (27) from MG1655 genomic DNA. An NdeI site was engineered into the forward primer and a SacI site into the reverse primer (underlined above), which, following enzymic digestion, allowed the 684 bp product to be ligated into pET28a (Novagen). The translated protein is produced with an N-terminal His-tag and thrombin cleavage site. This allowed the protein to be purified using TALON metal affinity resin (Clontech), which uses immobilised Co^{2+} ions to trap polyhistidine-tags with high-affinity, followed by cleavage with thrombin to release the pure protein. Insertion of the correct fragment was verified by digestion with restriction endonucleases. pET28a containing the zinT gene fragment (pET28a-zinT) was used to transform E. coli over-expression strain BL21(DE3) pLysS and named strain RKP5466.

Over-expression and purification of recombinant ZinT – Strain RKP5466 was grown in LB containing kanamycin (50 μg/ml, to maintain pET28a-zinT) and chloramphenicol (34 μg/ml, to maintain pLysS) at 37 ^{o}C with shaking to an OD_{600} of 0.6, at which point IPTG was added to a final concentration of 1 mM. Cells were harvested after a further 4 h incubation. Pellets were stored at -80 ^{o}C for later use; a cell pellet derived from 1 l culture was re-suspended in approximately 15 ml of buffer P (50 mM Tris/MOPS, 100 mM KCl, pH 8) and sonicated on ice to break the cells. Cell debris was pelleted by centrifugation for 30 min at 12 000 × g at 4 ^{o}C, whereupon the supernatant was removed and further centrifuged for 15 min at 27 000 × g. The cleared lysate was then loaded into a 5 ml TALON resin column, washed with 50 ml buffer P, followed by 50 ml buffer P containing 20 mM imidazole. Thrombin (60-80 units in 3-4 ml buffer P) was pipetted onto the

column, allowed to soak into the resin and incubated overnight at room temperature. Ten 1-ml fractions were eluted using buffer P. Recombinant ZinT was determined to be >95% pure by sodium dodecyl sulphate-polyacrylamide gel electrophoresis (SDS-PAGE). Protein was quantified using its absorbance at 280 nm and the theoretical extinction coefficient of 35995 M^{-1} cm^{-1} (estimated using the web-based program ProtParam at ExPASy (http://ca.expasy.org/cgi-bin/protparam), which assumes that all cysteines in the protein appear as half-cysteines using information based on (28). The theoretical extinction coefficient is based on the protein sequence minus the periplasmic targeting sequence.

N-terminal protein sequencing – Following SDS-PAGE, purified YodA was blotted onto a polyvinylidene fluoride (PVDF) membrane. The fragment of interest was excised from the membrane and the sequence determined using an Applied Biosystems Procise 392 protein sequencer.

Assays of metal binding to purified ZinT - Purified recombinant ZinT was exchanged into buffer D (20 mM MOPS pH 7) using a PD-10 desalting column (GE Healthcare). ZinT (1 ml) was incubated with various concentrations of $ZnSO_4$•$7H_2O$ (ACS grade reagent) and/or $CdCl_2$•$2½H_2O$ (AnalaR grade) for 1 h at room temperature. The protein/metal mixture was then loaded onto a PD-10 column and eluted in 7 × 0.5 ml fractions using buffer D. Fractions were assayed for A_{280} and for metal content using ICP-AES. Quantification of some elements was below the LOD in a limited number of samples that do not affect the overall interpretation of the experiment. In these cases the value for the LOD was used for subsequent calculations and thus will be an over-estimation.

Mag-fura-2 binding experiments - Purified recombinant ZinT was exchanged into buffer M (140 mM NaCl, 20 mM Hepes, pH 7.4) using a PD-10 desalting column. Absorption spectra were collected using a Varian Cary 50 Bio UV-visible spectrophotometer at 37 ^oC. Buffer composition and experimental conditions were taken from Simons (1993). ZinT (500 µl; approximately 15 µM) was placed in a quartz cuvette and a spectrum taken from which the concentration of ZinT was determined. Difference spectra were recorded in which the reference sample was buffer M. Equimolar mag-fura-2 (MF; Molecular Probes, catalogue number M-1290) was then added. Aliquots of $ZnSO_4$•$7H_2O$ (ACS grade reagent) and/or $CdCl_2$•$2½H_2O$ (AnalaR grade) in buffer M were added, mixed and incubated for 1 min before collecting spectra. Equilibrium was established within 1 min of Zn^{2+} being added.

RESULTS

Creating Zn^{2+}-deficient conditions - Several precautions, based on normal analytical practice, and the findings of Kay (29) regarding Zn^{2+} contamination, were taken to ensure that culture vessels and medium were depleted of Zn^{2+} where necessary. Table 2 shows typical values for the amounts of various metals in GGM as analysed by ICP-AES. Both Zn^{2+}-depleted and -replete media show good correlation with the expected values. In various batches of medium analysed, Zn^{2+} concentrations in Zn^{2+}-depleted medium ranged from <0.001 to 0.004 mg l^{-1} (<15 to 60 nM Zn^{2+}). The variation in Zn^{2+}-depletion achieved is a result of the difficulty in excluding Zn^{2+} from all sources that come into contact with the medium and culture. Sodium was used as the exchanging ion on Chelex-100, but excess sodium was not detected in the medium following chelation (data not shown).

Growth in Zn^{2+}-depleted batch cultures - E. coli strain MG1655 was grown in GGM with or without Zn^{2+} (Fig. 1A). The Zn^{2+}-limited culture showed a lag in entering exponential phase and a semi-logarithmic analysis of growth (not shown) revealed that the Zn^{2+}-limited culture had an

increased doubling time (159.0 min) compared to the Zn^{2+}-replete culture (125.4 min) and reached a lower final OD. Since OD measurements may reflect cell size changes (30), samples were taken at the end of growth for electron microscopy but no discernible size difference was seen between E. coli cells grown with or without Zn^{2+} in GGM (not shown). Cells grown in GGM (+/- Zn^{2+}) were, however, smaller (length, width and volume) than cells grown in rich medium (LB), presumably due to a slower growth rate (31).

GGM contains EDTA, which prevents precipitation of the trace elements present. This is well-established and common practice (17). However, to investigate whether this EDTA was itself creating Zn^{2+} depletion, we cultured MG1655 in GGM with and without EDTA (Supp. Fig. 1). When grown in GGM without EDTA, MG1655 displayed a longer lag phase and reduced growth yield. The growth rate was also affected; the doubling time during exponential growth increased from 125.5 min (with EDTA) to 131.5 min (without EDTA). Thus, EDTA is not creating a state of "Zn^{2+}-depletion" but rather is a beneficial component of the medium.

As well as growing at a reduced rate, cells grown in Zn^{2+}-depleted medium had approximately 1.8- to 5.0-fold less cellular Zn^{2+} than those grown in Zn^{2+} replete medium (based on three separate experiments). For example, at the end of the growth curve shown in Fig. 1A, the cells cultured in Zn^{2+}-replete medium contained 1.12×10^{-5} mg Zn^{2+}/mg dry weight cells and the cells grown in Zn^{2+}-depleted medium contained 3.40×10^{-6} mg Zn^{2+}/mg dry weight cells (a 3.3-fold difference). Here, "cellular Zn" is defined as that which cannot be removed by three successive washes with 0.5% nitric acid. To verify the reliability of the metal analyses, elemental recoveries were calculated from these samples. Fig. 2 shows that, for cells grown in Zn^{2+}-replete medium, Zn^{2+} recovery was between 90 and 110%, and, for cells grown in Zn^{2+}-replete and Zn^{2+}-deplete medium, the recovery of Fe, Cu, Co and Mg was also between 90 and 110%. For these elements, therefore, the metal content in the washed pellet and the culture supernatant and the wash supernatants fully accounts for the metal initially added to the culture in the medium. However, this was not true for Zn^{2+} recovery in cells grown in Zn^{2+}-deficient medium. Zn^{2+} in these cells, together with that in the culture supernatant and wash supernatants, was 5-fold higher than the amount originally added to the culture in the medium. This suggests an avid Zn^{2+}-sequestering ability of cells cultured under limiting Zn^{2+} conditions. Details of the analyses of individual pellets, wash solutions, supernatants and media for Zn^{2+} are found in Supp. Table 1. We conclude that Zn^{2+} limitation can be achieved in batch culture without resorting to chelators despite effective bacterial Zn^{2+} scavenging mechanisms.

Cells grown in continuous culture "find" extra Zn^{2+} - To explore Zn^{2+} acquisition and localization at constant growth rates and defined conditions for a detailed transcriptomic study, E. coli strain MG1655 was grown in parallel glycerol-limited chemostats, one fed with medium that contained "adequate" Zn^{2+} and one that had been rigorously depleted of Zn^{2+}. For the majority of elements assayed (Fe, Cu, Co, Mg, Mo, K, Mg, Na, P, S), the percentage recoveries were 90-110% (data not shown). However, more Zn^{2+} was recovered from the cells grown in the Zn^{2+}-deficient chemostat than was originally added to the culture (Table 3), as in batch culture (Fig. 2). This is presumed to be due to active leaching from glassware or carry-over from the inoculum. Interestingly, this percentage markedly decreased with successive experiments in the same chemostat apparatus, suggesting that there is less Zn^{2+} able to be leached after repeated runs of culture in the same chemostat vessel (Table 3). Details of the analyses of

individual pellets, wash solutions, supernatants and media are found in Supp. Table 2.

Cells grown in the Zn^{2+}-deficient chemostat consistently contained less cellular Zn^{2+} than those grown in Zn^{2+}-replete medium (e.g. 2.94×10^{-5} mg Zn^{2+}/mg cells for cells grown in adequate Zn^{2+} and 0.536×10^{-5} mg Zn^{2+}/mg cells for cells harvested from run 5 of the Zn^{2+}-limited chemostat (a 5.5-fold decrease)).

Transcriptome changes induced by Zn^{2+} deficiency - The genome-wide mRNA changes of strain MG1655 grown in continuous culture with adequate or limiting Zn^{2+} were probed using microarray technology. Commonly applied criteria to determine significance in transcriptomic studies are a fold-change of more than two and a P value of less than 0.05. Using these criteria, of the 4288 genes arrayed, only nine showed significant changes (an increase in all cases) in mRNA levels and are listed in Table 4. Genes not meeting these criteria may be biologically significant but are not studied further here. It should be noted that microarrays measure relative abundance of mRNA but cannot inform as to whether changes occur because of changes in the rate of transcription or because of changes in the stability of the transcript. Zn^{2+} has been reported to affect the stability of the mRNA of a human Zn^{2+} transporter (32). The full dataset has been deposited in GEO (accession number GSE11894) (33). Three genes were chosen for further study based on known links to Zn^{2+} homeostasis. The remaining six genes were not studied further. In total, 21 genes displayed a greater than two-fold increase in mRNA levels, 13 displayed a decrease and the mRNA changes from 140 genes had a P value of <0.05. No genes exhibited a two-fold or greater decrease in mRNA levels with a P value of less than 0.05.

The gene exhibiting the greatest change in transcription (and lowest P value) was zinT (up-regulated 8.07-fold), previously known as yodA. ZinT was initially identified in a global study of E. coli defective in the histone-like nucleoid-structuring protein H-NS (34). Levels of ZinT increase when cells are grown in the presence of Cd^{2+} (27), and at pH 5.8 (35). More recently, it has been suggested that the abundance of yodA mRNA changes in response to cytoplasmic pH stress (36). Transcription of zinT is increased by the addition of Cd^{2+}, but not Zn^{2+}, Cu^{2+}, Co^{2+} and Ni^{2+}, to growing cells (25), even though Cd^{2+}, Zn^{2+} and Ni^{2+} were found in crystals of ZinT (37,38) (see discussion). Further evidence for the binding of Cd^{2+} to ZinT was presented by Stojnev et al. (39), who found that γ-labelled $^{109}Cd^{2+}$-bound proteins could be detected in wild-type E. coli but not a mutant lacking zinT (39), suggesting a specific role for ZinT in Cd^{2+} accumulation. ZinT is found primarily in the cytoplasm in unstressed cells but is exported to the periplasm upon Cd^{2+} stress (25). The mature, periplasmic form of ZinT is thought to form a disulfide bond, as it is a substrate of DsbA (40). A recent paper (9) suggests a role for ZinT in periplasmic zinc binding under zinc-limiting conditions but no direct evidence for zinT up-regulation in response to rigorous exclusion of zinc has been previously reported.

The znuA gene was also up-regulated in response to Zn^{2+} depletion (Table 4). ZnuA is the soluble periplasmic metallochaperone component of the ZnuABC Zn^{2+} importer and was up-regulated 2.88-fold. In this complex, ZnuB is the integral membrane protein and ZnuC is the ATPase component. The znuB and znuC genes were up-regulated by 1.34- and 1.36-fold respectively (with P values of >0.05 and thus are not shown in Table 4). No other genes that encode proteins involved in Zn^{2+} transport (specifically zupT, zur, zitB, zntA, zntR, zraS, zraR, zraP) were more than 1.4-fold up-regulated or 1.2-fold down-regulated and all had P values of >0.05. The changes in the mRNA levels of a number of genes involved in Zn^{2+} metabolism are shown in Table 5.

The ykgM gene was up-regulated 2.64-fold in this study (Table 4) and has been identified previously by bioinformatics as the non-Zn^{2+}-ribbon-containing paralogue of the ribosomal protein L31 that normally contains a Zn^{2+}-ribbon motif and is thus predicted to bind Zn^{2+} (41). Panina et al. (41) predicted (but did not show) that ykgM would be up-regulated upon Zn^{2+} starvation and then displace the Zn^{2+}-containing version of L31 in the ribosome, thus liberating Zn^{2+} for use by Zn^{2+}-containing enzymes. However, no previous study has attained the degree of Zn^{2+} limitation reported here and the role of ykgM has not been further explored.

To verify the results obtained by microarray experiments, several genes that were induced by Zn^{2+} depletion were examined by qRT-PCR to determine independently relative mRNA levels. The levels of up-regulation determined by qRT-PCR (mean ± normalised standard deviation) were as follows: yodA, 7.77 ± 0.63; ykgM, 2.83 ± 0.61; and znuA, 2.34 ± 0.58. These values correspond closely to increases in the microarray analysis of 8.07-, 2.64-, 2.88-fold respectively. Similar qRT-PCR values were obtained on one (ykgM and znuA) or two (yodA) other occasions. The mRNA levels of holB (internal control) were unchanged as determined by qRT-PCR and array analysis.

Hypersensitivity of selected strains to Zn^{2+} deficiency - To assess the importance of the ykgM, zinT and znuA genes in surviving Zn^{2+} deficiency, mutants were used in which each gene are inactivated by insertion of an antibiotic resistance cassette; the growth of these isogenic strains was compared in Zn^{2+}-depleted and Zn^{2+} replete liquid cultures (Fig. 1). Each strain (wild-type and mutants) grew more poorly in the absence of Zn^{2+} than in its presence. Also, in Zn^{2+}-depleted medium, the ykgM::kan, zinT::cam and znuA::kan mutants consistently grew more poorly than MG1655 in the same medium. We were unable to culture the znuA::kan mutant to >5 Klett units in the severely Zn^{2+}-depleted conditions achieved here (Fig. 1D). All experiments were carried out in triplicate and similar results were seen on at least two separate occasions. We confirmed by qRT-PCR that the genes downstream of ykgM, zinT and znuA (i.e. ykgO, yodB and yebA, respectively) were in all cases transcribed in the mutant strains.

We measured cellular Zn^{2+} levels in bacteria grown in conditions of severe Zn^{2+} limitation in batch culture. The levels of Zn^{2+} detected in cell digests on analysis by ICP-AES were exceedingly low. Nevertheless, the zinT::cam strain contained approximately 9-fold less cellular Zn^{2+} when cultured under Zn^{2+} limitation (1.28×10^{-6} mg Zn^{2+}/mg cells) than when grown in Zn^{2+}-replete (1.16×10^{-5} mg Zn^{2+}/mg cells) conditions. Also, under Zn^{2+}-deficient conditions, the zinT::cam strain contained nearly 3-fold less cellular Zn^{2+} than MG1655 wild-type cells grown under similar conditions (1.28×10^{-6} mg Zn^{2+}/mg cells and 3.40×10^{-6} mg Zn^{2+}/mg cells, respectively). These data are the first to demonstrate a role for ZinT in Zn^{2+} acquisition under strictly Zn^{2+}-limited conditions. When the znuA::kan mutant was assayed after growth in Zn^{2+} depleted conditions, the measurement of cellular Zn^{2+} was below the LOD. Similar results were seen on at least one other occasion.

Transcriptional regulation of zinT under various Zn^{2+} concentrations - Having established that zinT transcription was elevated on Zn^{2+} depletion, a $P_{zinT\text{-}lacZ}$ transcriptional fusion (25), in which lacZ is transcribed from the zinT promoter, was used to investigate an alternative Zn^{2+} removal method and the effects of added Cd^{2+} and Zn^{2+}. Fig. 3A shows that $\lambda\Phi(P_{zinT}\text{-}lacZ)$ activity was highly up-regulated under the Zn^{2+}-deficient conditions created here (in which Zn^{2+} is excluded from the medium). These data were compared with cultures treated with TPEN (Fig. 3B), which is widely used as a Zn^{2+} chelator (e.g. (3,7,42-45)). Fig. 3B

shows that expression from λΦ (P_{zinT}-lacZ) increases with increasing TPEN concentrations in the growth medium. Although expression from λΦ (P_{zinT}-lacZ) was higher in cells grown in medium containing TPEN than in cells grown in adequate Zn^{2+}, it was lower than that of cells grown in medium from which Zn^{2+} has been rigorously eliminated (Fig. 3A). In LB medium, the P_{zinT}-lacZ fusion strain has previously been shown to respond to elevated levels of Cd^{2+} but not of Zn^{2+} (25). In GGM, the construct was again unresponsive to elevated Zn^{2+} but no response was seen to elevated Cd^{2+} (Fig. 3A), although this may be due to difficulties in growing cells at high levels of Cd^{2+}, which were near its maximum permissive concentration.

A Zur-binding site has been reported in the zinT promoter (41), and Zn^{2+}-bound Zur represses the transcription of znuABC (8). Therefore, to test the hypothesis that Zur also negatively-regulates zinT, λΦ(P_{zinT}-lacZ) activity was monitored in a strain lacking zur. Fig. 3C-D shows that, in a zur mutant, λΦ(P_{zinT}-lacZ) activity was not dependent on the extracellular Zn^{2+} concentration under any condition tested. Thus, Zur is a negative regulator of zinT transcription.

Stoichiometric binding of Zn^{2+} and Cd^{2+} by ZinT - To investigate the possible role of ZinT in metal binding as suggested by the transcription and growth studies reported here, the zinT gene was cloned into pET28a such that the translated protein lacked the periplasmic signal sequence but was fused to a polyhistidine tag and thrombin cleavage site to aid purification. The polyhistidine tag was removed by cleavage with thrombin to minimise the danger of the protein adopting aberrant conformations. The sequence of the resultant protein, which was used to calculate the extinction coefficient, mimics the form of the protein found in the periplasm. Residual imidazole in the final ZinT preparation was avoided by using only a single wash step containing imidazole (20 mM) during purification, and exchange into a buffer lacking imidazole before final use. Effective removal of the polyhistidine tag was confirmed by N-terminal sequencing. The pure recombinant protein (Fig. 4A) was incubated with different molar ratios of Zn^{2+}, and then subjected to size exclusion chromatography to assess co-elution of Zn^{2+} with ZinT. Fig. 4 shows the elution profiles of ZinT and Zn^{2+} following incubation of ZinT with 0, 0.25, 0.5, 1 and 2 molar equivalents of Zn^{2+}. Fig. 4B (and Fig. 5A-D) shows that, even when no Zn^{2+} is added, ZinT co-eluted from the size exclusion column with Zn^{2+}. The occupancy of Zn^{2+} observed under these conditions (0.6 mol Zn^{2+}/mol ZinT) was approximately half that observed at super-stoichiometric Zn^{2+}/ZinT ratios (Fig. 4F) and so we conclude that the Zn^{2+} content shown in Fig. 4B represents approximately 0.5 Zn^{2+} per ZinT. This suggests a high affinity of ZinT for Zn^{2+} and is reminiscent of the crystallisation of ZinT (38): crystals formed in the absence of added metals contained Zn^{2+} or Ni^{2+}, indicative of high metal affinity (see Discussion). When ZinT was incubated with 0.25 or 0.5 molar equivalents of Zn^{2+} (Fig. 4C-D) more Zn^{2+} co-eluted with ZinT than was originally added. However, when 1 (Fig. 4E), 2 (Fig. 4F) or 3 (data not shown) molar equivalents Zn^{2+} were incubated with ZinT, approximately one equivalent eluted from the column with the protein. These data provide evidence that ZinT binds 1 Zn^{2+} ion with high affinity.

Previous work (38) has suggested that ZinT is able to bind Cd^{2+} and so the experiment was also carried out using Cd^{2+}. ZinT co-elutes from a size exclusion column with up to 1 molar equivalent of Cd^{2+}, even when initially incubated with more (Fig. 5A-D). When 13.3 nmol ZinT was incubated without Cd^{2+} prior to size exclusion chromatography, the eluate contained less than 18 pmol Cd^{2+} per fraction (not shown). It should be noted that, in the case of Cd^{2+}, the Cd^{2+}/ZinT ratio was approximately 0.9 but never

exceeded 1 (Fig. 5D) unlike the case with Zn^{2+} (Fig. 4F). This is attributable to the inevitable contamination of reagents and materials with Zn^{2+} but not Cd^{2+}.

To investigate competition of Zn^{2+} and Cd^{2+} for site(s) in ZinT, the protein was incubated with both metals and co-elution of metals and protein assayed. ZinT co-eluted with almost 1 molar equivalent of Zn^{2+} and approximately 0.5 molar equivalents of Cd^{2+} (Fig. 5E). These ratios were similar when the Cd^{2+}:Zn^{2+} ratio was increased to 2:1 (Fig. 5F), indicating that ZinT preferentially binds Zn^{2+} over Cd^{2+}. Multi-element analysis of the eluate also revealed approximately 0.5 molar equivalents of Co^{2+} with ZinT. This was seen in all experiments and the reasons for this are discussed below. Two metal ions per ZinT protein would match previous structural data (38).

Mag-fura-2 (MF) and ZinT competitive metal binding - To estimate the affinity of ZinT for Zn^{2+}, Mag-fura-2, a chromophore that binds Zn^{2+} in a 1:1 ratio (46) and with a K_d of 20 nM (47), was used. Its absorption maximum shifts from 366 nm to 325 nm on Zn^{2+} binding, which is accompanied by a decrease in its extinction coefficient from 29900 M^{-1} cm^{-1} (MF) to 1880 M^{-1} cm^{-1} (Zn^{2+}-MF) (46). Therefore Zn^{2+} binding to MF can be tracked by examining the absorbance at 366 nm (Fig. 6A). Fig. 6B shows a titration of a 1:1 ZinT:MF mixture (filled circles) and MF alone (open circles) with Zn^{2+}. When ZinT was not present, the ΔA_{366} decreased to zero when 1 molar equivalent of Zn^{2+} had been added. When ZinT was present, however, incremental additions of Zn^{2+} gave smaller decreases in MF absorbance reaching a plateau at 2 molar equivalents of Zn^{2+}. This provides good evidence that, although the affinity of ZinT for Zn^{2+} is not high enough to completely outstrip MF of Zn^{2+}, ZinT competes with MF for binding of Zn^{2+}. The K_d for Zn^{2+} binding by ZinT is therefore not less than 20 nM, but of an order that is able to compete with MF for Zn^{2+}.

MF also binds Cd^{2+} in a 1:1 ratio and has a K_d for Cd^{2+} of 126 nM (48). Addition of Cd^{2+} to MF and ZinT (Fig. 6C-D) elicited a smaller decrease in absorbance than with MF alone, again indicating the ability of ZinT to compete with MF for Cd^{2+}. Without protein, the decrease in absorbance at 366 nm plateaued at 1 molar equivalent of metal added whereas, when ZinT was present, this shifted to 2. These data together suggest that ZinT has one binding site for metal that can be occupied by Cd^{2+} or Zn^{2+} and that the site has a sufficiently low K_d to be able to compete with MF for these metals.

DISCUSSION

The manipulation of metal ion concentrations in biological systems, so that the consequences of metal excess and limitation may be studied, is a major challenge. Global responses to elevated levels of Ag^{2+}, Cd^{2+}, Cu^{2+}, Ni^{2+}, Zn^{2+} and As (14,49-54) have been reported. However, constituents of complex growth medium can bind to metal ions and result in the metal ion concentration available to the cells being orders of magnitude lower than that added (16). For the first time, we have grown Zn^{2+}-depleted E. coli in batch and chemostat culture in defined medium, without recourse to chelating agents, and defined the transcriptome associated with severe Zn^{2+} limitation. In batch culture, wild-type E. coli MG1655 cells grown in Zn^{2+}-depleted cultures showed an increased doubling time (Fig. 1A) and a reduction in Zn^{2+} content compared to Zn^{2+}-replete cultures. Thus, in the face of extreme Zn^{2+} depletion in the extracellular medium, homeostatic mechanisms ensure adequate cellular Zn contents.

Zn^{2+}-depleted medium was successfully prepared by eliminating Zn^{2+} during medium preparation and culture. In contrast, chelators can be unspecific, strip metals from exposed sites and increase the availability of certain metals (16). The major disadvantage of using chelators is

that the metal is still present in the medium to be picked up by proteins with a higher affinity for the metal than that exhibited by the chelator. For example, ZnuA is able to compete with EDTA for Zn^{2+} (6). Fig. 3A highlights the disadvantage of using chelators to study Zn^{2+} deficiency; the widely-used chelator TPEN was less effective than Zn^{2+} elimination, as judged by $\lambda\Phi(P_{zinT}$-lacZ) activity. Although neither are specific to Zn^{2+}, both TPEN and EDTA have been used in studies focussing on Zn^{2+}-depletion (see earlier references and (55)).

Fig. 2 and Table 3 show that cells grown in Zn^{2+}-depleted medium accumulate Zn^{2+} that cannot be accounted for by the medium constituents. Table 3 shows that the extent of leaching decreased with successive experiments in the same chemostat apparatus. The most likely explanation is that metal is actively leached from the glassware (flasks or chemostat vessel). Kay (29) notes that acid washing removes only surface Zn^{2+}, which can be replaced from deeper within the glass. Previous studies have shown that growing cells in medium deficient in one nutrient can lead to cells evolving mechanisms to increase uptake of that nutrient (56).

In contrast to (10), this study found only nine genes to be differentially regulated in response to Zn^{2+} starvation after careful metal avoidance and extraction. The small number of differentially-regulated genes suggests that, due to the ubiquity of Zn^{2+} in the environment, cells have not evolved elaborate mechanisms to cope with extreme Zn^{2+} deficiency. Interestingly, computational analysis found only three candidate Zur sites in the E. coli genome and these were immediately upstream of three genes identified here – zinT, ykgM and znuA (41).

There is a precedent in Bacillus for re-distribution of Zn^{2+} under conditions of Zn^{2+} starvation, involving the synthesis of non-Zn^{2+}-finger homologues of Zn^{2+}-binding ribosomal proteins. Makarova et al. (57) searched sequenced genomes and found that genes encoding some ribosomal proteins were present as two copies: one, designated C^+, contains a Zn^{2+}-binding motif and, a second, designated C^-, in which this motif is missing. In the case of the E. coli ribosomal protein L31, the C^+ form is encoded by rpmE and the C^- form by ykgM (41) identified in the present study. Based on the present results, we hypothesise that non-Zn^{2+}-containing L31 proteins displace the Zn^{2+}-containing form in ribosomes and subsequent degradation of the latter form would release Zn^{2+} for use by other proteins. The number of ribosomes in the cell would make this a significant Zn^{2+} reserve. Such a model has been experimentally proven for L31 proteins in Bacillus subtilis (58,59) and Streptomyces coelicolor (60,61).

The present study shows that zinT expression is increased most dramatically, not by Cd^{2+} addition as reported previously (27), but by Zn^{2+} removal. However, the present and past findings are reconciled by the fact that Cd^{2+} may displace other metals from enzymes, such as Zn^{2+} from alkaline phosphatase in E. coli (2,25), so that Cd^{2+} exposure mimics Zn^{2+} depletion. Panina et al. (41) reported a Zur-binding site in the zinT promoter. Monitoring expression from $\lambda\Phi(P_{zinT}$-lacZ) in a strain lacking zur showed constitutive de-repression, regardless of extracellular Zn^{2+} concentration, confirming that Zur is involved in the regulation of zinT (Fig. 3). This was also reported in an unpublished thesis cited in a review (62).

Based on the established link between ZinT and Cd^{2+}, David et al. (38) included the metal (20 mM) in crystallisation trials and obtained a crystal form distinct from that obtained under crystallisation conditions that included 200 mM Zn^{2+} or no added metal. The crystal structure reveals a principal metal-binding site (common to all crystallised forms) that binds one Cd^{2+} or two Zn^{2+} ions. Further metal ions are found at the protein surface at intermolecular, negatively-charged sites

formed by residues from neighbouring ZinT molecules. The crystal form prepared in the absence of exogenous metal also revealed one metal ion bound in the central, common, metal-binding site; this metal was positioned similarly to Cd^{2+} and coordinated by the three same His residues. The buried metal-binding site must be of high-affinity, since no divalent cations were included in crystallisation of the native form. The binding geometry suggests that the metal in the native form is Zn^{2+}, although contamination by Ni^{2+} from the affinity chromatography or other metal ions could not be excluded, and X-ray fluorescence suggested the presence of Ni^{2+}, albeit in an unusual distorted tetrahedral geometry. Fig. 5E-F show that, in our hands, approximately 0.5 molar equivalents Co^{2+} co-elute with the ZinT protein. It is likely that this Co^{2+} has been picked up from the TALON column used during purification, again providing evidence for a high affinity metal-binding site within ZinT. No Ni^{2+} was found in eluting samples (data not shown).

On the basis of the crystallography, David et al. (38) could not conclude which metal would bind to ZinT under physiological conditions. The present study shows clearly that ZinT binds both Zn^{2+} and Cd^{2+} with high affinity. The direct binding experiments (Fig. 5E-F) show that more Zn^{2+} remains bound to ZinT after size-exclusion chromatography than Cd^{2+}, providing evidence that Zn^{2+} binds to ZinT more tightly than Cd^{2+}. Also, the K_d of MF for Cd^{2+} is greater than for Zn^{2+}, so somewhat weaker binding by Cd^{2+} would not be detected in the Mag-Fura-2 competition experiments. Fig. 5E-F shows that more than 1 molar equivalent of metal can bind to the protein. This is consistent with the crystal structure proposed by David et al. (38) which suggests that at least two Zn^{2+} ions can bind in the vicinity of the high-affinity site, and that there is additional capacity for further Zn^{2+}, up to 4, although this may be due to intermolecular contacts formed during crystallization. The finding that one Zn^{2+} ion is needed to saturate the protein, as assessed by competition with Mag-Fura-2, is entirely consistent with the crystallographic data as this experiment can only report on metal binding to ZinT that is tighter than 20 nM. Although this site in ZinT accommodates different metal ions, the marked accumulation of zinT mRNA by extreme Zn^{2+} limitation strongly suggests that the physiological role of ZinT is ferrying Zn^{2+} ions in the periplasm. Indeed, David et al. (38) suggested that the binding of a second metal, possibly at a lower affinity site, could trigger a conformational change that promotes transport across the membrane or interaction with an unidentified ABC-type transporter. In support of this is the fact that ZinT shows sequence similarity to a number of periplasmic metal-binding receptors of ABC metal-transport systems that have been shown to bind Zn^{2+}.

In a recent paper (9), growth in media with various Zn^{2+} supplements, or none, was purported to show "dependence of the ΔzinT mutant strain on zinc for growth". Zn^{2+}-limited conditions were those in which reduced growth yields (OD_{595}) were observed relative to growth at 0.6-1 mM added Zn^{2+}. In defined medium containing less than 0.4 mM Zn^{2+}, the mutant grew to lower ODs after 10 h than the wild-type but, at high Zn^{2+} (0.6-1 mM), the zinT mutant grew to higher OD values than the wild-type strain. This is in conflict with the present work (Fig. 1A, C), which shows that the zinT mutant and wild-type strains grew similarly, even at only 60 nM Zn^{2+}. Surprisingly, Kershaw et al. (9) also found that even growth of the wild-type strain was impaired at low Zn^{2+} concentrations (0.4, 0.05 mM added Zn^{2+}); with no added Zn^{2+}, growth was barely detectable. The claim that E. coli shows a strict dependence on added Zn^{2+} is, to our knowledge, unprecedented in the literature. Considerations of biomass composition suggest that the Zn^{2+} concentration in the medium used by Kershaw et al. (9) (0.5 mg l^{-1}) should support growth to a yield of 2.5 g dry

weight l^{-1} (17), well in excess of the OD_{595} of approximately 0.5 or lower reported (9). Furthermore, inspection of the responses of both wild-type and zinT mutant strains to metals reveals that the experiments (9) to define the Zn^{2+} response were conducted at limiting Cu concentrations: the basic defined medium contained 0.62 μM Cu (0.1 mg $CuSO_4$ l^{-1}), approximately 1000-fold lower than the required Cu concentration for optimal growth of both strains. Similarly, experiments to define the Cu response were conducted at limiting Zn^{2+} concentrations: the basic defined medium contained 3.1 μM Zn^{2+} (0.5 mg $ZnSO_4$ l^{-1}), i.e. much lower than the concentration at which both strains showed reduced cell yield. These calculations may explain why the cell yields at saturating Cu concentrations (0.6–1.0 mM) were significantly lower than those at saturating Zn^{2+} concentrations (0.6 –1.0 mM). Thus, the data of Kershaw et al. (9) do not provide robust evidence that the zinT mutant shows a growth disadvantage at low Zn^{2+} ion concentrations and conflict with previous work demonstrating the exceedingly low Cu concentrations required for Cu-limited growth (3,63).

Kershaw et al. (9) reported that ZinT binds metal ions. Cd^{2+} binding was observed when Cd^{2+} was incubated with the protein in a 1:1 ratio (0.1 mM ZinT:0.1 mM Cd^{2+}), although the resolution of a peak corresponding to mass 22,450 (ZinT plus 1 Cd^{2+}) is poor. The mass of the ZinT-Cd peak varied by 2 Da (as did the mass of apo-ZinT). The authors were only able to detect binding of Zn^{2+} to ZinT when 5 or more molar equivalents were added, although their other experiments detected binding when ZinT was incubated with less than 0.1 molar equivalents of Zn^{2+}. In Fig. 4 and 5 of the present study, we show binding of Zn^{2+} to ZinT when no metal is added due to the high affinity of ZinT for contaminating Zn^{2+} in the buffers.

Beside the need to sense Zn^{2+} levels to maintain homeostasis for all cellular systems, lack of Zn^{2+} may be sensed by pathogens as indicative of entry into the host and, thus, trigger expression of virulence factors. Indeed, several studies in different bacteria have established that ZnuA or ZnuABC (or homologues) are required for bacterial replication in the infected host (see (55,64) amongst others).

In conclusion, we propose that, when cells are severely starved of Zn^{2+}, the response is to increase Zn^{2+} uptake into the cell and re-distribute non-essential Zn^{2+}. The rpmE gene expresses the Zn^{2+}-finger L31 protein that is incorporated into the ribosome. Upon Zn^{2+}-depletion, the ykgM-encoded L31 protein is expressed (probably de-repressed by Zur) and becomes preferentially bound to the ribosome (the exact mechanism is unclear), allowing Zn^{2+} within the rpmE-encoded L31 to be recycled. The physiological role of ZinT remains to be fully established, but it may function as a Zn^{2+} chaperone to the membrane-bound Zn^{2+} importer ZnuBC (or a different importer), or mediate direct transport from the periplasm to the cytoplasm. Zn^{2+} is the metal that binds most tightly. This study provides a new appreciation of the regulation of zinT and the role of ZinT in protecting cells from Zn^{2+} depletion.

REFERENCES

1. Berg, J. M., and Shi, Y. (1996) Science **271**, 1081-1085
2. Fraústo da Silva, J. J. R., and Williams, R. J. P. (2001) The biological chemistry of the elements: the inorganic chemistry of life, Oxford University Press, Oxford
3. Outten, C. E., and O'Halloran, T. V. (2001) Science **292**, 2488-2492
4. Andreini, C., Banci, L., Bertini, I., and Rosato, A. (2006) J Proteome Res **5**, 3173-3178
5. Blencowe, D. K., and Morby, A. P. (2003) FEMS Microbiol Rev **27**, 291-311

6. Berducci, G., Mazzetti, A. P., Rotilio, G., and Battistoni, A. (2004) FEBS Lett **569**, 289-292
7. Patzer, S. I., and Hantke, K. (1998) Mol Microbiol **28**, 1199-1210
8. Patzer, S. I., and Hantke, K. (2000) J Biol Chem **275**, 24321-24332
9. Kershaw, C. J., Brown, N. L., and Hobman, J. L. (2007) Biochem Biophys Res Commun **364**, 66-71
10. Sigdel, T. K., Easton, J. A., and Crowder, M. W. (2006) J Bacteriol **188**, 6709-6713
11. Hayes, A., Zhang, N., Wu, J., Butler, P. R., Hauser, N. C., Hoheisel, J. D., Lim, F. L., Sharrocks, A. D., and Oliver, S. G. (2002) Methods **26**, 281-290
12. Hoskisson, P. A., and Hobbs, G. (2005) Microbiology **151**, 3153-3159
13. Piper, M. D., Daran-Lapujade, P., Bro, C., Regenberg, B., Knudsen, S., Nielsen, J., and Pronk, J. T. (2002) J Biol Chem **277**, 37001-37008
14. Lee, L. J., Barrett, J. A., and Poole, R. K. (2005) J Bacteriol **187**, 1124-1134
15. Beard, S. J., Hashim, R., Membrillo-Hernandez, J., Hughes, M. N., and Poole, R. K. (1997) Mol Microbiol **25**, 883-891
16. Hughes, M. N., and Poole, R. K. (1991) J GenMicrobiol **137**, 725-734
17. Pirt, S. J. (1975) Principles of Microbe and Cell Cultivation, Blackwell Scientific Publications, Oxford
18. Ferenci, T. (2007) Adv Microb Physiol **53**, 169-315
19. Garland, P. B., and Randle, P. J. (1962) Nature **196**, 987-988
20. Cherny, R. A., Atwood, C. S., Xilinas, M. E., Gray, D. N., Jones, W. D., McLean, C. A., Barnham, K. J., Volitakis, I., Fraser, F. W., Kim, Y., Huang, X., Goldstein, L. E., Moir, R. D., Lim, J. T., Beyreuther, K., Zheng, H., Tanzi, R. E., Masters, C. L., and Bush, A. I. (2001) Neuron **30**, 665-676
21. Lin, P. S., Kwock, L., Hefter, K., and Misslbeck, G. (1983) Cancer Res **43**, 1049-1053
22. Mukherjee, G., and Ghosh, T. (1995) J Inorg Biochem **59**, 827-833
23. Sebat, J. L., Paszczynski, A. J., Cortese, M. S., and Crawford, R. L. (2001) Appl Environ Microbiol **67**, 3934-3942
24. Datsenko, K. A., and Wanner, B. L. (2000) Proc Natl Acad Sci U S A **97**, 6640-6645
25. Puškárová, A., Ferianc, P., Kormanec, J., Homerova, D., Farewell, A., and Nystrom, T. (2002) Microbiology **148**, 3801-3811
26. Miller, J. H. (1972) Experiments in Molecular Genetics, Cold Spring Harbor Laboratory Press
27. Ferianc, P., Farewell, A., and Nystrom, T. (1998) Microbiology **144**, 1045-1050
28. Gill, S. C., and von Hippel, P. H. (1989) Anal Biochem **182**, 319-326
29. Kay, A. R. (2004) BMC Physiol **4**, 4
30. Koch, A. L. (1961) Biochim Biophys Acta **51**, 429-441
31. Neidhardt, F. C., Ingraham, J. L., and Schaechter, M. (1990) Physiology of the Bacterial Cell: a Molecular Approach, Sinauer Associates, Inc, Sunderland, Massachusetts
32. Jackson, K. A., Helston, R. M., McKay, J. A., O'Neill, E. D., Mathers, J. C., and Ford, D. (2007) J Biol Chem **282**, 10423-10431
33. Barrett, T., Troup, D. B., Wilhite, S. E., Ledoux, P., Rudnev, D., Evangelista, C., Kim, I. F., Soboleva, A., Tomashevsky, M., and Edgar, R. (2007) Nucleic Acids Res **35**, D760-765
34. Laurent-Winter, C., Ngo, S., Danchin, A., and Bertin, P. (1997) Eur J Biochem **244**, 767-773
35. Birch, R. M., O'Byrne, C., Booth, I. R., and Cash, P. (2003) Proteomics **3**, 764-776
36. Kannan, G., Wilks, J. C., Fitzgerald, D. M., Jones, B. D., Bondurant, S. S., and Slonczewski, J. L. (2008) BMC Microbiol **8**, 37
37. David, G., Blondeau, K., Renouard, M., and Lewit-Bentley, A. (2002) Acta Crystallogr D Biol Crystallogr **58**, 1243-1245

38. David, G., Blondeau, K., Schiltz, M., Penel, S., and Lewit-Bentley, A. (2003) J Biol Chem **278**, 43728-43735
39. Stojnev, T., Harichova, J., Ferianc, P., and Nystrom, T. (2007) Curr Microbiol **55**, 99-104
40. Kadokura, H., Tian, H., Zander, T., Bardwell, J. C., and Beckwith, J. (2004) Science **303**, 534-537
41. Panina, E. M., Mironov, A. A., and Gelfand, M. S. (2003) Proc Natl Acad Sci U S A **100**, 9912-9917
42. Cai, F., Adrion, C. B., and Keller, J. E. (2006) Infect Immun **74**, 5617-5624
43. Fekkes, P., de Wit, J. G., Boorsma, A., Friesen, R. H., and Driessen, A. J. (1999) Biochemistry **38**, 5111-5116
44. Jackson, K. A., Helston, R. M., McKay, J. A., O'Neill E, D., Mathers, J. C., and Ford, D. (2007) J Biol Chem **282**, 10423-10431
45. Scott, C., Rawsthorne, H., Upadhyay, M., Shearman, C. A., Gasson, M. J., Guest, J. R., and Green, J. (2000) FEMS Microbiol Lett **192**, 85-89
46. Yatsunyk, L. A., Easton, J. A., Kim, L. R., Sugarbaker, S. A., Bennett, B., Breece, R. M., Vorontsov, II, Tierney, D. L., Crowder, M. W., and Rosenzweig, A. C. (2008) J Biol Inorg Chem **13**, 271-288
47. Simons, T. J. (1993) J Biochem Biophys Methods **27**, 25-37
48. de Seny, D., Heinz, U., Wommer, S., Kiefer, M., Meyer-Klaucke, W., Galleni, M., Frere, J. M., Bauer, R., and Adolph, H. W. (2001) J Biol Chem **276**, 45065-45078
49. Brocklehurst, K. R., and Morby, A. P. (2000) Microbiology **146 (Pt 9)**, 2277-2282
50. Kershaw, C. J., Brown, N. L., Constantinidou, C., Patel, M. D., and Hobman, J. L. (2005) Microbiology **151**, 1187-1198
51. Moore, C. M., Gaballa, A., Hui, M., Ye, R. W., and Helmann, J. D. (2005) Mol Microbiol **57**, 27-40
52. Wang, A., and Crowley, D. E. (2005) J Bacteriol **187**, 3259-3266
53. Yamamoto, K., and Ishihama, A. (2005) Mol Microbiol **56**, 215-227
54. Yamamoto, K., and Ishihama, A. (2005) J Bacteriol **187**, 6333-6340
55. Davis, L. M., Kakuda, T., and DiRita, V. J. (2009) J Bacteriol **191**, 1631-1640
56. Notley-McRobb, L., and Ferenci, T. (1999) Environ Microbiol **1**, 45-52
57. Makarova, K. S., Ponomarev, V. A., and Koonin, E. V. (2001) Genome Biol **2**, RESEARCH 0033
58. Akanuma, G., Nanamiya, H., Natori, Y., Nomura, N., and Kawamura, F. (2006) J Bacteriol **188**, 2715-2720
59. Nanamiya, H., Akanuma, G., Natori, Y., Murayama, R., Kosono, S., Kudo, T., Kobayashi, K., Ogasawara, N., Park, S. M., Ochi, K., and Kawamura, F. (2004) Mol Microbiol **52**, 273-283
60. Owen, G. A., Pascoe, B., Kallifidas, D., and Paget, M. S. (2007) J Bacteriol **189**, 4078-4086
61. Shin, J. H., Oh, S. Y., Kim, S. J., and Roe, J. H. (2007) J Bacteriol **189**, 4070-4077
62. Hantke, K. (2005) Curr Opin Microbiol **8**, 196-202
63. Ciccognani, D. T., Hughes, M. N., and Poole, R. K. (1992) FEMS Microbiol Lett **73**, 1-6
64. Ammendola, S., Pasquali, P., Pistoia, C., Petrucci, P., Petrarca, P., Rotilio, G., and Battistoni, A. (2007) Infect Immun **75**, 5867-5876

FOOTNOTES

This work was supported by the Biotechnology and Biological Sciences Research Council BBSRC, UK. We thank Dr. A. J. G. Moir (Krebs Sequencing and Synthesis Facility, University of Sheffield, UK) for carrying out the N-terminal protein sequencing.

The abbreviations used are: Amp^r, ampicillin resistant; cam, chloramphenicol-resistance cassette; ICP-AES, inductively coupled plasma-atomic emission spectroscopy; kan, kanamycin-resistance cassette; LB, Luria-Bertani medium; LOD, limit of detection; MES, 2-(N-morpholino)ethanesulfonic acid; MF, mag-fura-2; PAGE, polyacrylamide gel electrophoresis; PTFE, polytetrafluoroethylene (Teflon®); PVC, polyvinyl chloride; PVDF, polyvinylidene fluoride; qRT-PCR, quantitative real-time-polymerase chain reaction; SDS, sodium dodecyl sulphate; Spc^r spectinomycin-resistance cassette; TPEN, N, N, N`, N`-tetrakis(2-pyridylmethyl)ethylenediamine.

FIGURE LEGENDS

Fig. 1. Growth of wild-type and isogenic mutant E. coli strains in Zn^{2+}-depleted (filled circles, solid line) and Zn^{2+} replete (open circles, dashed line) GGM in batch culture. In each case, means and standard deviations of three flasks are plotted. The doubling times (min) of the strains during exponential growth, calculated from semi-logarithmic plots, were as follows: MG1655 replete, 125; MG1655 deplete, 159; ykgM::kan replete, 211; ykgM::kan deplete, 885; zinT::cam replete, 124; zinT::cam replete, 193; znuA::kan replete 134; znuA::kan deplete, 492. A) MG1655 wild-type; B) ykgM::kan (FB20133); C) zinT::cam (RKP5456); D) znuA::kan (FB23354).

Fig. 2. Recovery of elements following growth of strain MG1655 in batch culture. The means and standard deviations of three flasks are plotted. Black and grey bars represent the percentage of added elements recovered from cells grown in Zn^{2+}-replete and -deplete conditions, respectively. See text for details of calculation.

Fig. 3. β-galactosidase activity of $\lambda\Phi(P_{zinT}$-lacZ) under various conditions. A) and B) β-galactosidase activity of $\lambda\Phi(P_{zinT}$-lacZ) (strain AL6) grown in GGM containing the concentrations of Zn^{2+}, Cd^{2+} and TPEN shown. The Zn^{2+} concentrations can be interpreted as follows: 6.14 μM is GGM in which the bulk elements were Chelex-100-treated and then trace elements containing Zn^{2+} were added back; <0.06 μM is GGM in which extreme precautions were taken to exclude Zn^{2+} (see text). Cultures were harvested when the OD_{600} reached 0.2 - 0.4. The mean +/- standard deviation for three technical replicates is shown. The same results were seen on at least one other occasion. C) and D) β-galactosidase activity of $\lambda\Phi(P_{zinT}$-lacZ) in a zur::Spc^r background (strain RKP5475) grown in GGM containing the Zn^{2+} and TPEN concentrations shown. Cultures were harvested with the OD_{600} reached 0.2 - 0.4. The means and standard deviations of three technical replicates are shown. The same results were seen on at least one other occasion.

Fig. 4. Metal binding to purified ZinT. A) Purified recombinant ZinT (right lane) on an SDS-PAGE gel. Size markers (left lane) are shown in kDa. Elution profiles of ZinT and Zn^{2+} from a PD-10 column following incubation of protein and metal ions. B) Elution following incubation of 13.3 nmol ZinT with no added metal. C) – F) Elution following incubation of 28.6 nmol ZinT with 0.25, 0.5, 1 or 2 molar equivalents of Zn^{2+}. Filled circles with solid line, ZinT; open circles with dashed line, Zn^{2+}.

Fig. 5. Elution profiles of ZinT, Zn^{2+} and Cd^{2+} from a PD-10 column following incubation of protein and metal ions. A) – D) Elution following incubation of 17.8 nmol ZinT with 0.5, 1, 2 or

3 molar equivalents of Cd^{2+}. Filled circles with solid line, ZinT; open circles with dashed line, Zn^{2+}; open triangles with dotted line, Cd^{2+}. E) – F) Elution following incubation of 13.3 nmol ZinT with 1 molar equivalent of Zn^{2+} and 1 molar equivalent of Cd^{2+} or with 1 molar equivalent of Zn^{2+} and two molar equivalents of Cd^{2+}. Filled circles with solid line, ZinT; open circles with dashed line, Zn^{2+}; open diamonds with dotted and dashed line, Co^{2+}; open triangles with dotted line, Cd^{2+}.

Fig. 6. Titration of ZinT and/or MF with Zn^{2+} and/or Cd^{2+}. A) Representative difference spectra (i.e. minus the protein-only spectrum) of a titration of 14.5 μM ZinT and 14.5 μM MF with Zn^{2+} (0.25 to 3.5 molar equivalents Zn^{2+} in 0.25 steps, then 4 to 6 molar equivalents in 0.5 steps). Arrows indicate the direction of absorbance changes as Zn^{2+} is added. B) Titration of 14.5 μM ZinT and 14.5 μM MF with Zn^{2+}. C) Titration of 14.3 μM ZinT and 14.3 μM MF with 1 molar equivalent of Cd^{2+}, then Zn^{2+} in 0.5 molar equivalent steps to 4 molar equivalents, then Zn^{2+} in 0.5 molar equivalent steps to 6 molar equivalents. D) Titration of 14.1 μM ZinT and 14.1 μM MF with 2 molar equivalents of Cd^{2+}, then Zn^{2+} in 0.5 molar equivalent steps. In B) – D), absorbance change at 366 nm is plotted against molar equivalents of metal added. Filled circles are in the presence of ZinT; open circles are in the absence of ZinT (MF and buffer only). Lines indicate whether the added metal was Zn^{2+} or Cd^{2+}.

Table 1. List of strains used.

Strain	Genotype	Source
AL6	MC4100 λΦ(P_{zinT}-lacZ)	(25)
FB20133	MG1655 ykgM::kan	UW Genome Project
FB23354	MG1655 znuA::kan	UW Genome Project
MC4100	F^- araD139 Δ(argF-lac)U169 rpsL150 relA1 flbB5301 deoC1 ptsF25 rbsR	(25)
MG1655	F^- λ^- ilvG rfb-50 rph-1	Laboratory stock
SIP812	MC4100 zur::Spc^r	(8)
RKP5082	MG1655/pKD46 (Amp^r)	This work
RKP5456	MG1655 zinT::cam	This work
RKP5466	BL21(DE3) pLysS pET28a-zinT	This work
RKP5475	AL6 with zur::Spc^r	This work

Table 2. Expected and representative measured amounts of elements in Zn^{2+}-sufficient and -depleted GGM.

Element	predicted from medium composition (mg l^{-1})	measured by ICP-AES (mg l^{-1})	
		Zn^{2+}-sufficient	Zn^{2+}-depleted
Zn	0.401/0 (+Zn/-Zn)	0.340	0.004
Fe	1.045	0.886	0.878
Cu	0.037	0.033	0.034
Co	0.0257	0.018	0.019
Mo	0.054	0.068	0.059
Ca	2.24	2.83	2.85
Mg	24	24.2	25.0

Table 3. Recovery of Zn^{2+} from E. coli strain MG1655 growing in a Zn^{2+}-limited chemostat (run 1) followed by successive cultures in the same chemostat under the same conditions (runs 2-5). A "run" is an experiment conducted after terminating a chemostat experiment and re-establishing a new culture in the same apparatus. ND, not determined. See text for details of calculation.

Run	Recovery (%) of Zn^{2+} in medium			
	Washed cell pellet + wash solutions + supernatant		Unwashed cell pellet + supernatant	
	+Zn	-Zn	+Zn	-Zn
1	104	1858	ND	ND
2	110	1676	ND	ND
3	105	559	ND	ND
4	104	493	102	454
5	103	248	103	254

Table 4. Genes with a significant change in mRNA level in response to Zn^{2+}-deficiency. Only genes with a fold increase of more than 2 and a P value of less than 0.05 are included. Gene names are the primary names on Ecogene (www.ecogene.org). Gene descriptions are from Ecogene.

Gene	b number	Gene product	Fold increase	P value (<0.05)
zinT	b1973	Periplasmic cadmium binding protein; induced by cadmium and peroxide; binds zinc, nickel, cadmium; SoxS and Fur regulated	8.07	0.0001
znuA	b1857	High-affinity ABC transport system for zinc, periplasmic	2.88	0.00117
fdnG	b1474	Formate dehydrogenase-N, selenopeptide, anaerobic; periplasmic	2.86	0.00386
emtA	b1193	Membrane-bound transglycosylase E, lipoprotein; involved in limited murein hydrolysis	2.86	0.00998
ykgM	b0296	RpmE paralog, function unknown	2.64	0.03647
mdtD	b2077	Putative transporter, function unknown; no MDR phenotype when mutated or cloned; fourth gene in mdtABCDbaeRS operon	2.46	0.01614
ribA	b1277	GTP cyclohydrolase II, riboflavin biosynthesis	2.36	0.02506
ydfE	b1577	Pseudogene, N-terminal fragment, Qin prophage	2.17	0.00452
aslA	b3801	Suppresses gpp mutants; putative arylsulfatase	2.15	0.02660

Table 5. Changes in the mRNA levels from a number of genes in response to Zn^{2+}-deficiency. Gene names are the primary names on Ecogene (www.ecogene.org). Gene descriptions are from Ecogene.

Gene	b number	Gene product	Fold change	P value
yodB	b1974	Function unknown	2.38	0.0725
zur	b4046	Repressor for znuABC, the zinc high-affinity transport genes; dimer; binds two Zn(II) ions per monomer	1.37	0.9578
znuC	b1858	High-affinity ABC transport system for zinc	1.36	0.2294
znuB	b1859	High-affinity ABC transport system for zinc	1.34	*
zntR	b3292	Zn-responsive activator of zntA transcription	1.34	0.4857
zraS	b4003	Two component sensor kinase for ZraP; responsive to Zn^{2+} and Pb^{2+} ; autoregulated; regulation of Hyd-3 activity is probably due to crosstalk of overexpressed protein	1.32	0.1109
zraP	b4002	Zn-binding periplasmic protein; responsive to Zn^{2+} and Pb^{2+} ; regulated by zraSR two-component system; rpoN-dependent	1.25	0.9322
yiiP	b3915	Iron and zinc efflux membrane transporter; cation diffusion facilitator family; dimeric	1.17	0.2742
zitB	b0752	Zn(II) efflux transporter; zinc-inducible	1.09	0.9571
zntA	b3469	Zn(II), Cd(II), and Pb(II) translocating P-type ATPase; mutant is hypersensitive to Zn^{2+} and Cd^{2+} salts	1.07	0.9285
spy	b1743	Periplasmic protein induced by zinc and envelope stress, part of cpxR and baeSR regulons	1.03	0.8314
zraR	b4004	Two component response regulator for zraP; responsive to Zn^{2+} and Pb^{2+} ; autoregulated; regulation of Hyd-3 activity is probably due to crosstalk of overexpressed protein	0.95	0.9315
zupT	b3040	Zinc and other divalent cation uptake transporter	0.88	0.3258

* Insufficient data available to obtain a P value.

Figure 1

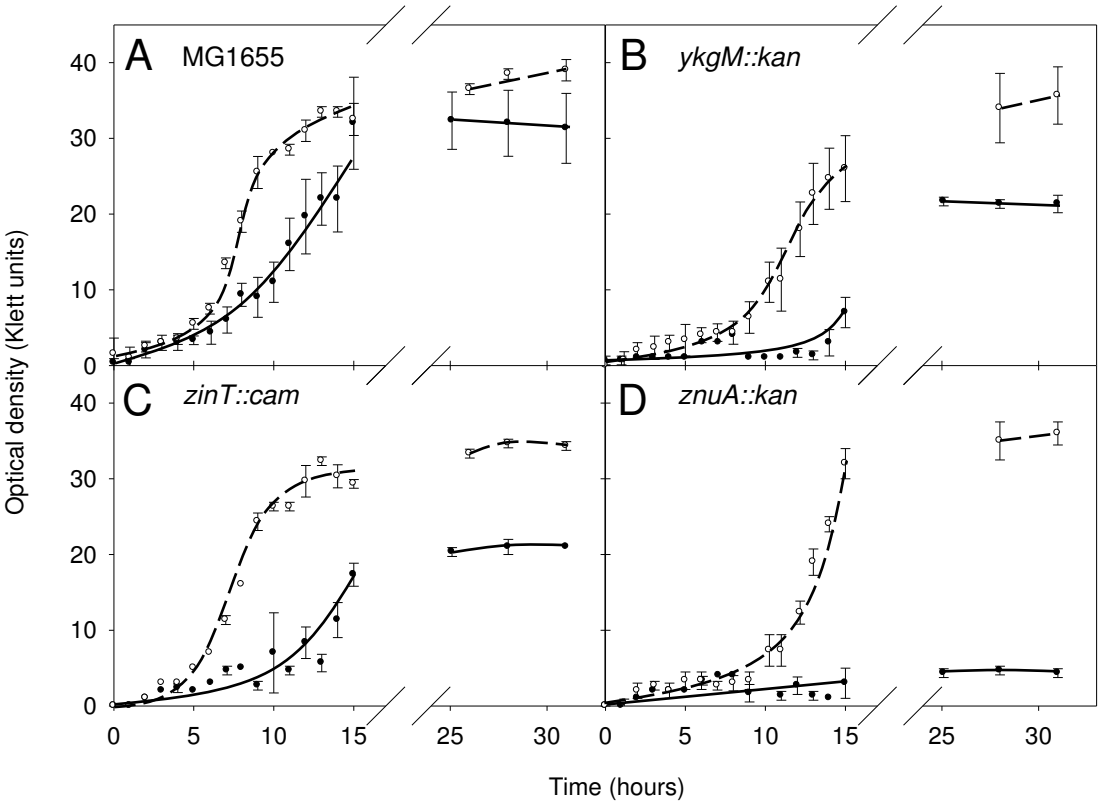
A MG1655
B ykgM::kan
C zinT::cam
D znuA::kan
Optical density (Klett units)
Time (hours)
0
10
20
30
40
0
5
10
15
25
30

Figure 2

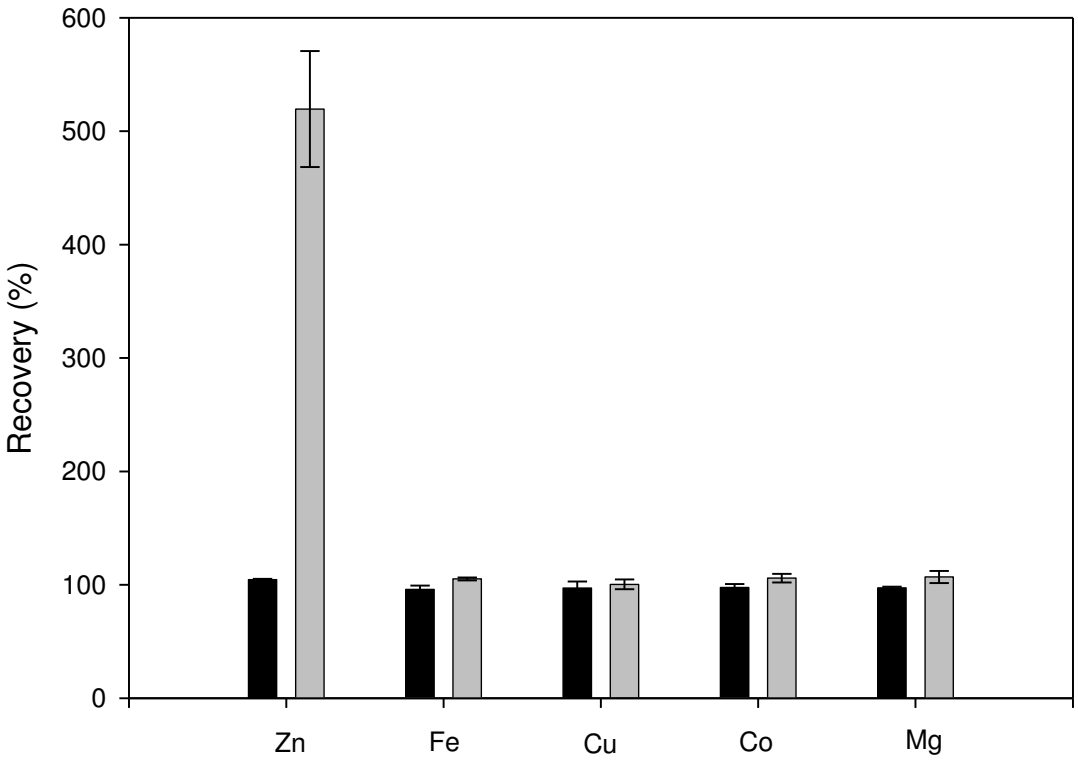

Figure 3

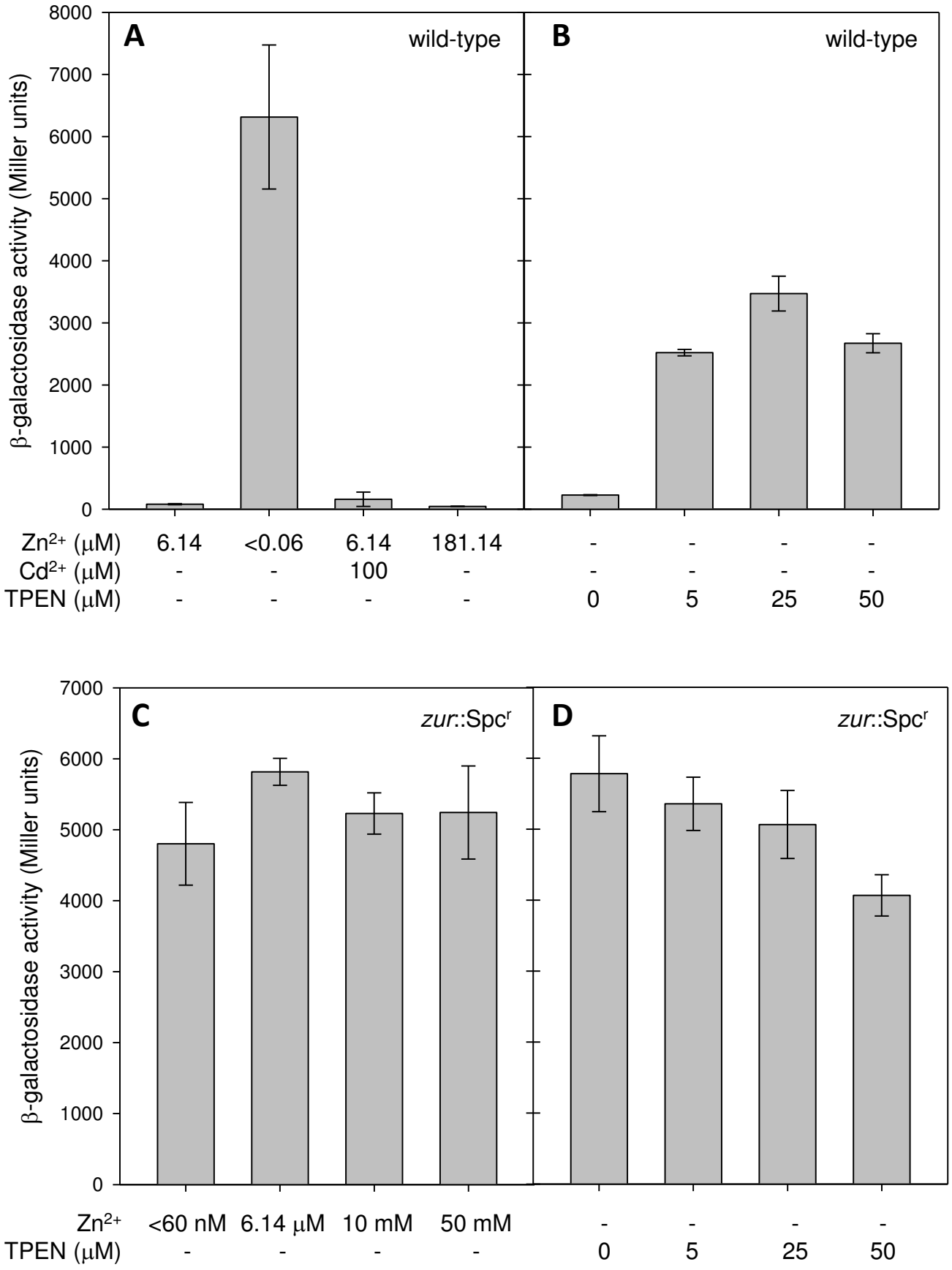
A
wild-type
B
wild-type
β-galactosidase activity (Miller units)
8000
7000
6000
5000
4000
3000
2000
1000
0
Zn2+ (μM) 6.14 <0.06 6.14 181.14 - - - -
Cd2+ (μM) - - 100 - - - - -
TPEN (μM) - - - - 0 5 25 50
C
zur::Spcr
D
zur::Spcr
β-galactosidase activity (Miller units)
7000
6000
5000
4000
3000
2000
1000
0
Zn2+ <60 nM 6.14 μM 10 mM 50 mM - - - -
TPEN (μM) - - - - 0 5 25 50

Figure 4

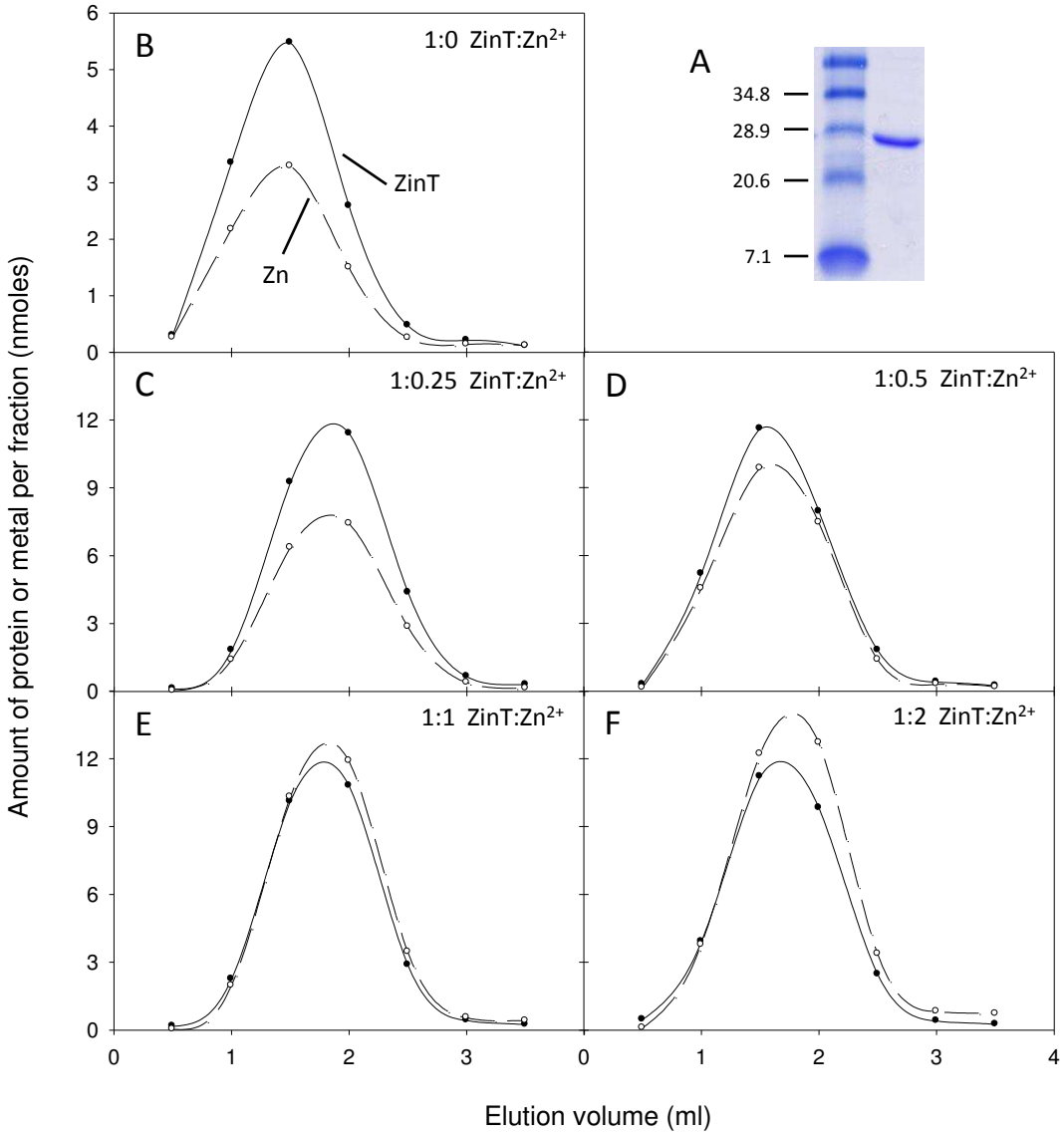
A
34.8
28.9
20.6
7.1
B
1:0 ZinT:Zn2+
ZinT
Zn
C
1:0.25 ZinT:Zn2+
D
1:0.5 ZinT:Zn2+
E
1:1 ZinT:Zn2+
F
1:2 ZinT:Zn2+
Amount of protein or metal per fraction (nmoles)
Elution volume (ml)

Figure 5

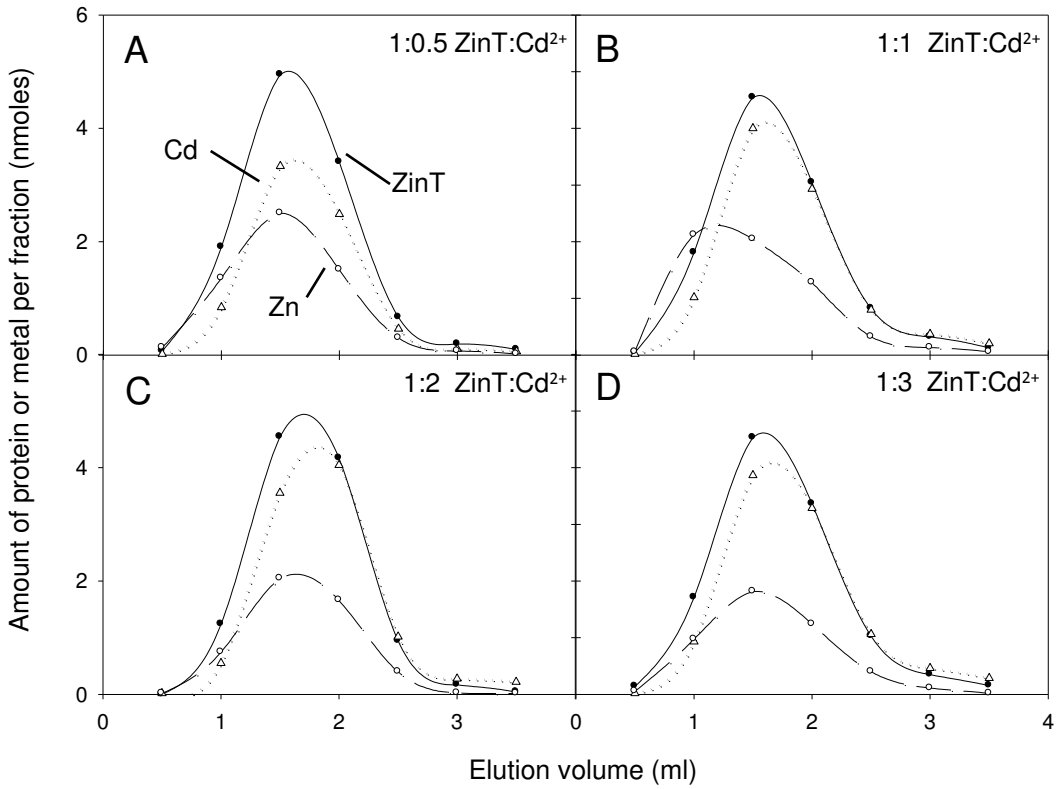
A
1:0.5 ZinT:Cd2+
B
1:1 ZinT:Cd2+
C
1:2 ZinT:Cd2+
D
1:3 ZinT:Cd2+
Cd
ZinT
Zn
Amount of protein or metal per fraction (nmoles)
Elution volume (ml)

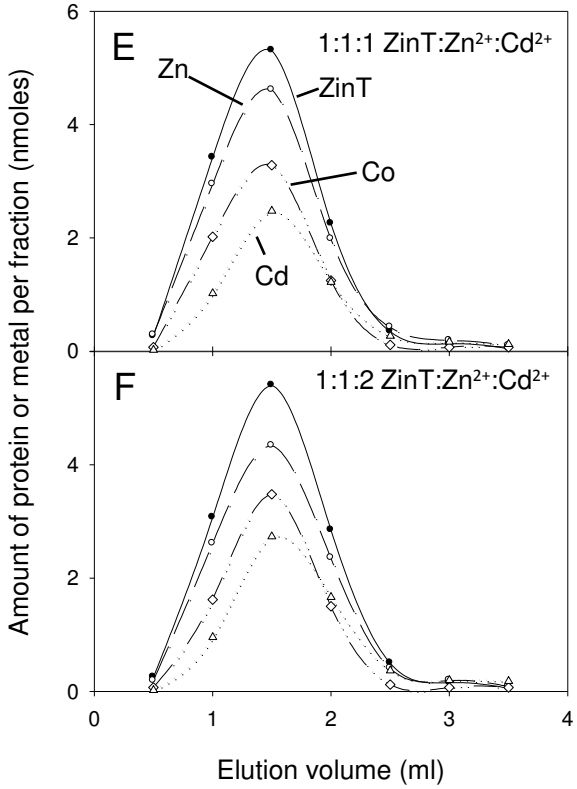
E
1:1:1 ZinT:Zn2+:Cd2+
Zn
ZinT
Co
Cd
F
1:1:2 ZinT:Zn2+:Cd2+
Amount of protein or metal per fraction (nmoles)
Elution volume (ml)

Figure 6

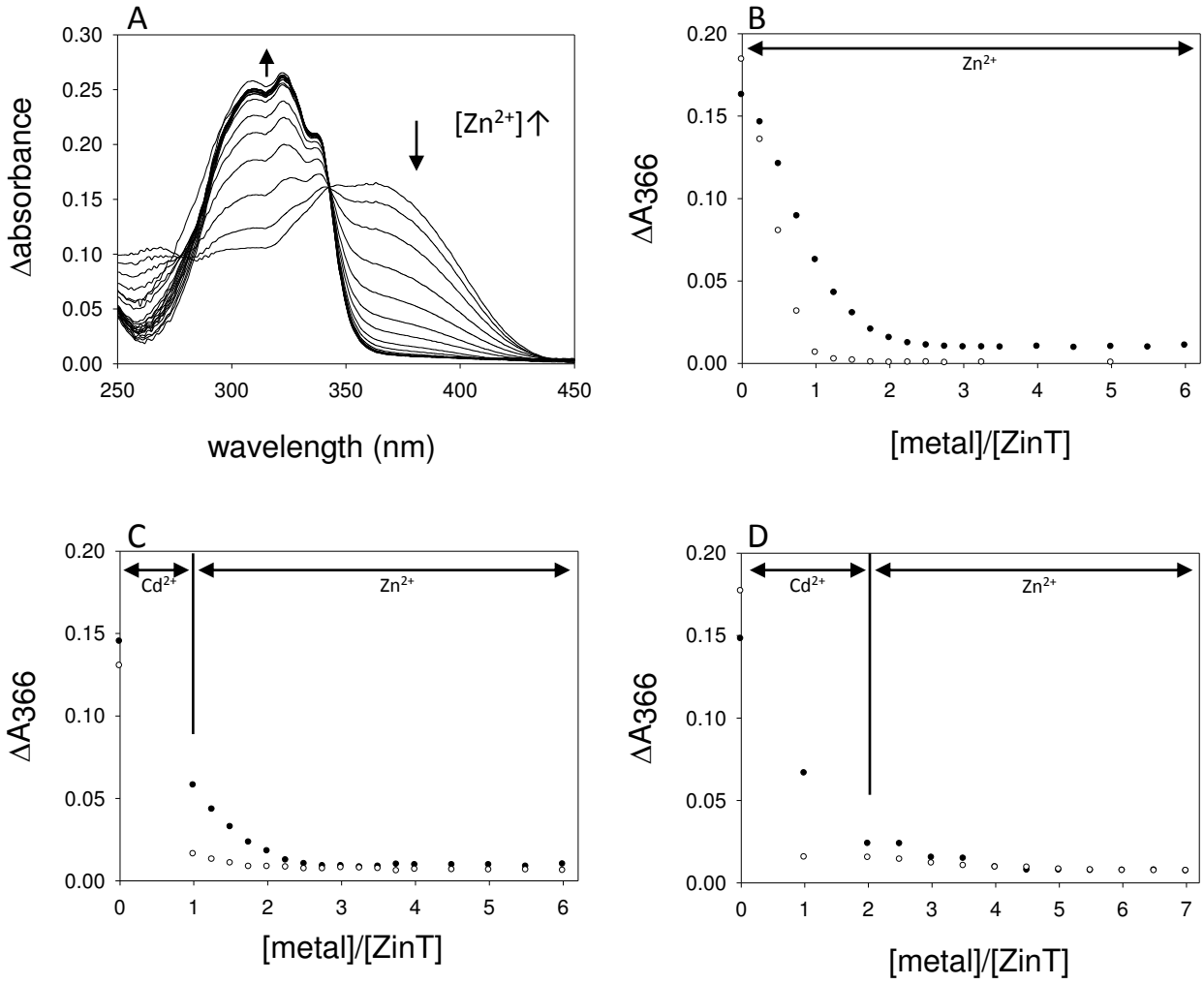
A
Δabsorbance
wavelength (nm)
[Zn2+]↑
B
ΔA366
[metal]/[ZinT]
Zn2+
C
ΔA366
[metal]/[ZinT]
Cd2+
Zn2+
D
ΔA366
[metal]/[ZinT]
Cd2+
Zn2+